Title

Glucocorticoids activate a synapse weakening pathway culminating in tau phosphorylation in the hippocampus

Authors

Jee Hyun Yi[a,e], Christopher Brown[a,b,e], Garry Whitehead[a], Thomas Piers[a,b,c], Young Seok Lee[a,d], Celia Martinez Perez[a], Philip Regan[a,c], Daniel J. Whitcomb[a,c] and *Kwangwook Cho[a,c]

Affiliations

[a] Henry Wellcome Laboratories for Integrative Neuroscience and Endocrinology, School of Clinical Sciences, Faculty of Health Sciences, University of Bristol, Whitson Street, Bristol, BS1 3NY, United Kingdom

[b] Chonnam-Bristol Frontier Laboratory, Biomedical Research Institute, Chonnam National University Hospital, Gwangju 501-757, South Korea

[c] Centre for Synaptic Plasticity, University of Bristol, Whitson Street, Bristol, BS1 3NY, United Kingdom

[d] Department of Life Sciences, Imperial College, London, SW7 2AZ, United Kingdom

[e] These authors contributed equally to the work.

Corresponding Author

Kwangwook Cho, Henry Wellcome Laboratories for Integrative Neuroscience and Endocrinology, Whitson Street, Bristol, BS1 3NY, United Kingdom. Email: kei.cho@bristol.ac.uk

Abstract

Evidence suggests that the stress hormones glucocorticoids (GCs) can cause cognitive deficits and neurodegeneration. Previous studies have found GCs facilitate physiological synapse weakening, termed long-term depression (LTD), though the precise mechanisms underlying this are poorly understood. Here we show that GCs activate glycogen synthase kinase-3 (GSK-3), a kinase crucial to synapse weakening signals. Critically, this ultimately leads to phosphorylation of the microtubule associated protein tau, specifically at the serine 396 residue, and this is a causal factor in the GC-mediated impairment of synaptic function. These findings reveal the link between GCs and synapse weakening signals, and the potential for stress-induced priming of neurodegeneration. This could have important implications for our understanding of how stress can lead to neurodegenerative disease.

Keywords: Glucocorticoids; Long-term potentiation; GSK-3; Tau

1. Introduction

Repeated and chronic stress can cause acceleration of brain ageing, memory deficits and various mental illnesses [1,2]. Rising levels of the stress hormone cortisol are strongly correlated with temporal lobe atrophy and cognitive deficits during ageing in humans [2]. These effects are prevalent in patients with hypercortisolism [3,4] and can even be mirrored in otherwise healthy individuals by repeated exposure to environmental stressors such as jet lag [5]. It has been reported that prolonged secretion of glucocorticoids (GCs) during chronic stress, or exogenous application of GCs, disrupts memory performance in both humans [6,7] and rodents [8-10]. Understanding the precise mechanisms underpinning how elevated-GCs cause both cognitive deficits and structural atrophy in the brain remains a major scientific challenge with numerous translational implications.

Several rodent studies have demonstrated that stress and GCs inhibit long-term potentiation (LTP) but enhance long-term depression (LTD) [11,12]. Given the postulated role for these synaptic phenomena in learning and memory [13], it is likely that their dysregulation is central to the cognitive impairments induced by GCs. Although the activation of glucocorticoid receptors (GRs) triggers a wide variety of intracellular signals [14-16], the synaptic signalling pathways that underlie aberrant synapse weakening by GCs remain to be elucidated.

Based on the aforementioned findings, one possibility is that GCs regulate the direction of plasticity and/or the fate of synapses via modulation of certain signalling pathways involved in LTD, or synapse weakening. A key molecule linking synapse weakening and disruption of LTP expression is glycogen synthase kinase-3 (GSK-3) [17]. Our previous studies also implicate caspase-3-induced cleavage of Akt1 as a

critical factor for the expression of physiological LTD [18], and suggest that it acts as an upstream regulator of GSK-3 to enhance LTD in amyloid-beta (Aβ)-mediated pathophysiological conditions [19]. Furthermore, GSK-3 orchestrates this synapse weakening mechanism through regulation of tau phosphorylation (pTau) [20,21]. Given the key role of aberrant pTau in the pathophysiology of Alzheimer's disease and stress-mediated neurodegeneration [22-24], we hypothesise that GSK-3-mediated signalling pathways leading to pTau could be a synapse weakening mechanism common to these diseased states.

Here we provide evidence that GCs activate a synapse weakening signal pathway centred around the cleavage of Akt1 by caspase-3 and subsequent activation of GSK-3, which causes aberrant pTau and abolishes LTP expression in the rat hippocampus. We identify a single pTau residue (Ser396) as a critical downstream signal in this mechanism, resulting in GC-mediated aberrant synaptic weakening. These findings could provide further translation to our understanding of how GCs prime progressive neurodegeneration through aberrant functional plasticity in the hippocampus.

2. Materials and Methods

2.1. Animals

Experiments involving animals were conducted in accordance with the UK Animals Scientific Procedures Act, 1986 and associated guidelines. All experimental protocols were approved by the University of Bristol Animal Welfare & Ethical Review Body. Male Wistar rats (Charles River, UK) were used to prepare organotypic (7-day-old rats) and acute hippocampal slices (4- to 5-week-old rats). Rats were housed four or five per cage, and were allowed access to water and food

ad libitum. The cages were maintained at a constant temperature (23 ± 1°C) and relative humidity (60 ± 10%) under a 14/10 hour light-dark cycle (lights on from 8:00 A.M.).

2.2. Electrophysiology

2.2.1. Acute hippocampal slice field recording

Animals were sacrificed from 9:00 - 10:00AM by cervical dislocation. Brains were quickly removed into ice-cold artificial cerebrospinal fluid (ACSF; 124mM NaCl, 3mM KCl, 26mM $NaHCO_3$, 1.25mM NaH_2PO_4, 2mM $CaCl_2$, 1mM $MgSO_4$, 10mM D-glucose, carbogenated with 95% O_2 / 5% CO_2). Hemispheres were separated with a midsagittal cut and hippocampi were micro-dissected from each intact hemisphere. Transverse hippocampal slices (400 µm) were cut using a Mcllwain tissue chopper (Mickle Laboratory Engineering) and allowed to recover in a submersion-type bath filled with ACSF for at least 60 minutes. Before recording, hippocampal slices were incubated in ACSF with pharmacological compounds at room temperature. Evoked field excitatory postsynaptic potentials (fEPSPs) were recorded in the CA1 region using glass electrodes containing NaCl (3 M). Stimulating electrodes placed in the subiculum and CA2 region (Schaffer collateral pathway). Stimuli were delivered alternately to the two electrodes at a baseline rate of 0.066 Hz. Stimulus intensity was set at 30-40% of saturating intensity. After 30 minutes of stable baseline, high-frequency stimulation (2 × 100 pulses; 100 Hz, 30 s interval) was used for the LTP induction protocol. LTP was gauged as the change of fEPSP slope relative to the preconditioning baseline. Both control and experimental recordings were collected using slices prepared from the same animal. Analysis of control LTP data across all field recording experiments showed no significant difference between mean post-

conditioning fEPSPs in slices prepared from different rats (one-way ANOVA, $F(4,33) = 2.147$, $p = 0.097$). Data were captured and analysed using LTP114j software. Data are expressed relative to a normalized baseline. For analyses, the baseline was defined as 5 points before tetanic stimulation and the post-conditioning time was set at 75-80 minutes following recording commencement. The difference between baseline and post-conditioning time-points was expressed as a percentage of baseline ± SEM, and was used to make comparisons between treatment groups.

2.2.2. Hippocampal slice culture and biolistic transfection

Organotypic slices were cultured based upon a method previously described by Stoppini *et al*. (1991) [25]. Briefly, rats were decapitated, and their brains rapidly removed and placed into ice-cold dissecting medium containing: 238 mM sucrose, 2.5 mM KCl, 26 mM $NaHCO_3$, 1 mM NaH2PO4, 5 mM $MgCl_2$, 11 mM D-glucose, and 1 mM $CaCl_2$. Hippocampi were extracted, and transverse hippocampal slices (350 µm thickness) were cut and placed upon sterile, semi-porous membranes. These were stored and maintained at the interface between air and culture medium (containing: 78.8% Mimimum Essential Medium, 20% heat-inactivated horse serum, 30 mM HEPES, 26 mM D-glucose, 5.8 mM $NaHCO_3$, 2 mM $CaCl_2$, 2 mM $MgSO_4$, 70 µM ascorbic acid, 1 µg/ml insulin, pH 7.3 and 320 – 330 mOsm/kg) inside a humidified incubator at 35°C with a 5% CO_2-enriched atmosphere. Culture medium was refreshed every 2 days, and slices were used for whole-cell recording at 6 – 8 days *in vitro* (DIV).

DNA-coated microcarriers for biolistic transfection of organotypic hippocampal slices were prepared based on previously described methods [26]. At DIV 3–5, neurons

were transfected with plasmids expressing shRNA against rat tau protein (OriGene Technologies). A mixture of four different tau shRNA constructs (1:1:1:1, in pGFP-V-RS vector) was used for tau silencing. Phosphorylation-null (serine residues mutated to alanine) human tau constructs of the AT8 [S199, S202, threonine 205 (T205)] and PHF-1 (S396, S404) epitopes, in pCI-neo vectors, were kindly provided by Dr. A. Takashima (Department of Aging Neurobiology, National Center for Geriatrics and Gerontology, Obu, Japan). Individual mutations to the PHF-1 epitope (residues S396 or S404) were generated by site-directed mutagenesis (Agilent Technologies) of 2N4R human tau. Wild-type and triple mutant Akt1 (D108A/D119A/D462N) were generated as previously described [18].

2.2.3. Whole–cell patch clamp recording

For whole-cell recordings from cultured organotypic slices, the recording chamber was perfused with a buffer solution containing 119 mM NaCl, 2.5 mM KCl, 4 mM $CaCl_2$, 4 mM $MgCl_2$, 26 mM $NaHCO_3$, 1 mM NaH_2PO_4, 11 mM glucose, 0.02 mM picrotoxin, and 0.01 mM 2-chloroadenosine. The buffer solution was maintained at 29–30°C and saturated with 95% O_2/5% CO_2. Recording electrodes (5–6 MΩ) containing $CsMeSO_4$ filling solution (130 mM $CsMeSO_4$, 8 mM NaCl, 4 mM Mg-ATP, 0.3 mM Na-GTP, 0.5 mM EGTA, 10 mM HEPES, and 6 mM QX-314, pH 7.2–7.3 and 270 –290 mOsm/kg) were used to voltage clamp CA1 pyramidal neurons. EPSCs were recorded at a holding voltage of −70 mV, and only cells that had an initial Rs (series resistance) < 20 MΩ that was maintained within 20% of that value from start to finish were included in final data analysis. To induce LTP, depolarization of the cell to 0 mV was paired with 200 pulses of 2 Hz stimulation to the Schaffer collateral

input. Analysis of control LTP data across all whole cell patch recording experiments showed no variation in interleaved control LTP levels over time and in different slices (one-way ANOVA, $F(4,11) = 1.775$, $p = 0.230$). The change in peak amplitude of the EPSC, relative to baseline, was used to assess the effects of these stimulation protocols on synaptic efficacy. For analysis purposes, the baseline was defined as 5 points before 2 Hz stimulation and the post-conditioning time was set as the last 5 points at the 40-minute time-point. The difference between baseline and post-conditioning time-points was expressed as a percentage of baseline ± SEM, and was used to make comparisons between treatment groups.

2.3. Western Blotting and Antibodies

Hippocampal slices were collected and homogenised in lysis buffer (1% SDS, 292mM sucrose, 2.6mM EDTA, 1:10 Protease Inhibitor Cocktail (Sigma Aldrich), 1:100 Phosphatase Inhibitor Cocktail 3 (Sigma Aldrich)).

For immunoblotting, primary antibodies were used at the following dilutions: anti-phospho-GSK-3β Ser9 (rabbit polyclonal, Cell Signalling Technology, 1:500), anti-GSK-3β (H-76) (rabbit polyclonal, Santa Cruz Biotechnology, 1:500), anti-phospho-Akt1 Ser473 (rabbit polyclonal, Cell Signalling, 1:1000), anti-phospho-Akt1 Thr308 (rabbit polyclonal, Cell Signalling, 1:1000), anti-Akt1 (rabbit polyclonal, Cell Signalling, 1:1000), anti-PHF-1 (mouse monoclonal, kindly provided by Dr. P. Davies, 1:1000), anti-phospho-Tau Ser396 (rabbit polyclonal, Life Technologies, 1:1000), anti-phospho-Tau Ser404 (rabbit polyclonal, Life Technologies, 1:1000), anti-phospho-PHF-tau pSer202+Thr205 (AT8) (Mouse monoclonal, Thermo

Scientific, 1:1000), anti-Tau 5 (mouse monoclonal, Life Technologies, 1:1000), anti-β-Actin (mouse monoclonal, Abcam, 1:10,000).

Membranes were incubated in horseradish peroxidase–conjugated secondary antibodies at the following dilutions: anti-rabbit (goat polyclonal, Millipore, 1:5000), anti-mouse (goat polyclonal, Millipore, 1:5000), followed by imaging with the G:Box gel imaging system (Syngene) using the EZ-ECL detection system (Thermo Scientific Inc.). Optical densities of immunoreactive bands were measured using ImageJ software (NIH) and statistical analysis conducted with SigmaPlot (Systat Software, Inc., USA). Example blots were cropped around regions of interest for presentation in figures. For quantitative comparisons of treatment groups, optical densities for proteins of interest were normalized to loading-control protein levels and expressed relative to the average value from the control group.

2.4. Akt1 kinase assay

Akt1 activity was determined as described by the manufacturer's instructions (Cell Signalling), with minor modifications. Acute hippocampal slices were washed with TBS and homogenised in IP buffer (25 mM Tris pH 7.5, 150 mM NaCl, 1 % Triton X-100, 1 mM EDTA, 1 mM EGTA, 1 mM PMSF, 1 mM Na-Orthavanadate, 1X phosphatase inhibitors and 1X Protease inhibitors). Lysates were centrifuged at 15,000 g for 15 minutes at 4°C and the supernatant transferred to fresh tubes. Immunoprecipitation of Akt1 was performed using 500 µg of lysate and incubated with 2 µg of Akt1 Ser473 antibody overnight at 4°C. Subsequently, 30 µl of washed Protein G agarose slurry was added and incubated at 4°C for 45 minutes with over-end mixing. The beads were washed twice in IP buffer, followed by two washes in

NEB kinase buffer. The immobilised precipitated Akt1 was incubated in 40 µl kinase buffer containing 200 µM ATP and 1 µg of GSK3β fusion protein at 30°C for 30 minutes. The reaction was stopped by addition of 20 µl of 3X sample buffer. The samples were vortexed and centrifuged prior to heating and protein separation by SDS-PAGE.

2.5. Statistical analysis

Where practically possible, experiments were performed blind to experimental condition. Results are presented as the mean ± standard error of the mean (SEM). Results were analysed using unpaired *t*-test for two independent groups or by one-way ANOVAs with post-hoc Holm-Sidak analysis for multiple groups, as indicated in the results text and figure legends. $p < 0.05$ was considered statistically significant. N numbers represent samples from independent animals unless otherwise specified.

3. Results

3.1. GCs activate a synapse weakening pathway to inhibit LTP

In acutely prepared dorsal hippocampal slices, corticosterone (CORT; 1 µM) application for 2 hours (Ctrl: 146.12 ± 2.9%; CORT: 114.33 ± 5.6%, unpaired t-test $t(13) = 5.2$, $p < 0.001$, Fig. 1a), or application of the synthetic glucocorticoid dexamethasone (DEX; 200 nM, 2 hours, Ctrl: 164.35 ± 4.5%; DEX: 133.92 ± 3.9%, unpaired t-test, $t(12) = 4.9$, $p < 0.001$, Fig. 1b), both inhibited LTP induction when compared to untreated slices. No effects of CORT treatment on basal properties of synaptic transmission were observed (Supplementary Fig. S1). Based on previous

studies [18-21], we hypothesised that GCs activate a caspase-3-Akt1-GSK-3 signalling (CAG) cascade that induces aberrant expression of LTD and inhibits LTP. We therefore tested whether GC exposure impairs LTP via activation of this CAG cascade. Co-application of the GSK-3 inhibitor CT-99021 (1 μM) prevented the LTP impairment that was induced by CORT treatment alone (CORT: 114 ± 5.3%; CORT+CT-99021: 142.9 ± 3.8%, unpaired t-test, $t(10) = 3.1$, $p = 0.0114$, Fig. 1c), suggesting that GSK-3 activation is required for CORT-mediated inhibition of LTP. Furthermore, LTP impairment induced by CORT was prevented by the caspase inhibitor Z-DEVD-FMK (10 μM) but not by the non-active control peptide Z-FA-FMK (10 μM), supporting a role for caspase-3 upstream of GSK-3 activation in the aberrant modulation of synaptic plasticity (one-way ANOVA, $F(3,22) = 8.85$, $p = 0.003$; Holm-Sidak post hoc test for CORT+Z-DEVD-FMK (149.7 ± 6.4%, $p = 0.005$) and CORT+Z-FA-FMK (120.7 ± 5.2%, $p = 0.793$) vs CORT (118.5 ± 5.8%), Fig. 1d). Indeed, the activation of GSK-3 was robustly induced by CORT treatment and was prevented by pre-treatment (30 min) and co-application of Z-DEVD-FMK (one-way ANOVA, $F(3,36) = 14.41$, $p < 0.001$; Holm-Sidak post hoc test for CORT (56.7 ± 9.6%) vs CORT+Z-DEVD-FMK (89.1 ± 6.4%, $p = 0.031$), Fig. 1e). Z-FA-FMK had no effect on the CORT-induced activation of GSK-3β (CORT (56.7 ± 9.6%) vs CORT+Z-FA-FMK (58.8 ± 7.9 %, $p = 0.858$, Fig. 1e) and neither Z-DEVD-FMK nor Z-FA-FMK altered the total expression level of GSK-3β (one-way ANOVA, $F(3,39) = 0.09$, $p = 0.96$, Fig. 1e).

We also utilized a previously characterised XIAP Bir 1,2 protein, which inhibits caspase-3 and 7 activation [18]. XIAP Bir 1,2 was biolistically transfected into neurons of cultured hippocampal slices. In this cultured slice model, cells exposed to CORT treatment (200 nM, 24 hours) exhibited impaired LTP when compared to

untreated cells (untreated: 160.1 ± 14.0%; CORT: 93.7 ± 15.2%, unpaired t-test $t(8) = 3.2$, $p = 0.012$, Fig. 1f). This effect was dependent upon the presence of the GR, such that CORT failed to block LTP in neurons transfected with GR shRNA when compared to untransfected cells (untransfected: 85.7 ± 12.5%; GR-shRNA transfected: 157.3 ± 24.9 %, unpaired t-test $t(8) = 2.6$, $p = 0.033$, Fig. 1g). CORT treatment did not inhibit LTP in XIAP Bir1,2 overexpressing cells when compared to untransfected cells (untransfected: 103.6 ± 20.8%; XIAP Bir1,2 transfected: 169.5 ± 20.2%, unpaired t-test $t(11) = 2.3$, $p = 0.044$, Fig. 1h), indicating a requirement for caspase-3 / 7 activation for the inhibition of LTP by CORT. In line with our hypothesis, these results suggest that CORT induces both GSK-3 and caspase activation.

3.2. GCs inhibit LTP via Akt1 regulation

Since the mitochondrial permeability transition pore (mPTP) is important for the activation of caspases [27], we tested whether mPTP regulates CORT-induced LTP inhibition. The mPTP inhibitor TRO-19622 (25 μM) prevented both the CORT-mediated activation of GSK-3β (one-way ANOVA, $F(2,15) = 11.74$, $p = 0.003$; Holm-Sidak post hoc test for CORT+TRO-19622 (94.9 ± 6.9%, $p = 0.010$) vs CORT (69.7 ± 3.6%), Fig. 2a) and the inhibition of LTP (CORT: 114.3 ± 5.8%; CORT+TRO-19622: 144.1 ± 2.2%, unpaired t-test $t(11) = 6.5$, $p = 0.001$, Fig. 2b). These results imply that aberrant regulation of mPTP activates caspase and GSK-3, which subsequently dysregulate LTP. Since caspase-3 can regulate GSK-3 through cleavage of Akt1 [18,19], we hypothesised that the observed caspase mediated upregulation of GSK-3 activity might be due to Akt1 cleavage and that this is a key

sequential step in the inhibition of LTP. Previous findings have shown that phosphorylation of Akt1 modulates its cleavage in a site–specific manner [28]. We therefore measured the phosphorylation of Akt1 at Thr308, a site correlated with Akt1 cleavage and activity [29]. We found that Thr308 phosphorylation was significantly reduced by CORT treatment (one-way ANOVA, $F(3,20) = 10.13$, $p < 0.001$; Holm-Sidak post hoc test for CORT (42.2 ± 12.3%, $p = 0.024$) vs control (100.0 ± 13.0%), Fig. 2c) and that this reduction was prevented by pre-treating slices with either Z-DEVD-FMK or the GR antagonist RU486 (500 nM), (CORT vs CORT+Z-DEVD-FMK (142.6 ± 17.5%, $p < 0.001$), CORT vs CORT+RU486 (114.7 ± 8.9%, $p = 0.005$,Fig. 2c). The total expression of Akt1 was unaffected by CORT, Z-DEVD-FMK or RU486 (one-way ANOVA, $F(3,20) = 0.59$, $p = 0.632$, Fig. 2c). This suggests that CORT inhibits Akt1 activity via caspase activation, and is a specific consequence of GR activation. To further validate the effect of CORT on Akt1 activity, we used an *in vitro* kinase assay utilising immuno-precipitated Akt1 from control and CORT treated hippocampal slices and a GSK-3 fusion protein as a substrate to determine the activity of immobilised Akt1. We found that CORT treatment reduced Akt1 activity as observed by a significant decrease in phosphorylated GSKαβ at serine residues 21 and 9 (pGSKαβ Ser21/9) levels compared to control (control: 100.0 ± 8.44%; CORT: 73.9 ± 3.67%, unpaired t-test $t(4) = 7.1$, $p = 0.002$, Fig. 2d). We next aimed to determine whether caspase-3-mediated Akt1 cleavage is important for the inhibition of LTP by CORT. To do this, we biolistically transfected mutant Akt1 protein (Akt1 triple mutant, resistant to cleavage by caspase-3[18]) into CA1 hippocampal neurons. CORT treatment did not impair LTP in cells transfected with the Akt1 triple mutant when compared to untransfected cells (untransfected: 104.9 ± 7.2%; Akt1 triple mutant transfected;

144.8 ± 13.5%, unpaired t-test $t(9) = 2.5$, $p = 0.036$, Fig. 2e) but inhibited LTP in cells transfected with wild-type Akt1 (untransfected: 117.4 ± 11.7.%; Akt1 wild-type: 107.4 ± 16.3%, unpaired t-test $t(10) = 0.5$, $p = 0.628$, Fig. 2f).

3.3. GCs induce pTau specifically at the PHF-1 epitope

Together, these results suggest that CORT-mediated LTP inhibition relies upon the cleavage of Akt1 by caspase-3 and this might be a critical step to further downstream signal cascades which ultimately execute functional synapse weakening. What remains to be shown, however, are the potential downstream substrates that mediate synaptic weakening and dysregulate LTP. GSK-3 is a well-characterised kinase of the tau protein, governing the phosphorylation of tau (pTau) at multiple sites [30]. Interestingly, pTau at Ser396, one of the GSK-3 target sites closely associated with pathogenesis in AD [30], was recently revealed as necessary for LTD [21]. Given previous evidence showing increased pTau following stress [31], we postulated that CORT-induced activation of GSK-3, via upstream caspase-3-Akt1 regulation, might culminate in greater pTau and thus aberrant modulation of synaptic plasticity. Therefore, we tested whether caspase, mPTP and GSK-3 activation are involved in CORT-mediated changes to pTau. CORT treatment significantly increased immunoreactivity with the PHF-1 antibody, which detects pTau at amino acids Ser396 and Ser404 (S396/404) (one-way ANOVA, $F(3,20) = 4.83$, $p < 0.001$; Holm-Sidak post hoc test for control (100.0 ± 16.0%) vs CORT (135.9 ± 7.9%, $p = 0.001$, Fig. 3a), and this effect of CORT occurred in a caspase dependent manner (CORT vs CORT+Z-DEVD-FMK (90.4 ± 4.4%, $p < 0.001$, Fig. 3a). We also tested AT8, an antibody that detects alternate GSK-3 phosphorylation residues Ser-202 and Thr-205, and found no change in phosphorylation at these sites (one-way ANOVA, $F(3,20) = 0.43$, $p = 0.734$, Fig. 3b). The CORT-mediated increase in PHF-1

immunoreactivity was also prevented by co-treatment with an inhibitor of the mPTP ((one-way ANOVA, $F(2,15) = 9.96$, $p < 0.001$; Holm-Sidak post hoc test for control (100.0 ± 4.2%) vs CORT (139.7 ± 5.9%, $p = 0.003$), CORT vs CORT+TRO-19622 (88.2 ± 10.0%, $p < 0.001$, Fig. 3c) or an inhibitor of GSK-3 (139.8 ± 8.0%) vs CORT+CT-99021 (104.1 ± 10.4%, $p = 0.008$, Fig. 3e). AT8 immunoreactivity was again unchanged in both cases (one-way ANOVA, $F(2,15) = 0.58$, $p = 0.573$, Fig. 3D; one-way ANOVA, $F(2,24) = 0.38$, $p = 0.69$, Fig. 3f).These data show that CORT-triggered signalling cascades drive an increase in pTau, specifically at residues of the PHF-1 epitope.

3.4. CORT-induced inhibition of LTP is mediated by specific pTau at Ser396

Based on previous findings that pTau is required for LTD induction as well as Aβ-mediated LTP inhibition [21, 22], we were interested in determining whether CORT-induced LTP inhibition is due to aberrant synapse weakening mediated through pTau. To test this, endogenous tau was first knocked down by rat tau small hairpin-forming interference RNA (shRNA) in cultured hippocampal slices [21], allowing us to determine whether tau itself is critical to CORT-mediated LTP inhibition. Indeed, robust LTP was induced in rat tau shRNA transfected neurons, but not in untransfected neurons, that were treated with CORT (untransfected: 105.6 ± 17.9%; tau shRNA transfected: 162.9 ± 19.5%, unpaired t-test $t(12) = 2.4$, $p = 0.032$, Fig. 4a). In addition, neurons where endogenous tau was replaced with S396/404 residue phospho-null human tau (S396/404A) readily exhibited LTP following treatment with CORT when compared to untransfected cells (untransfected: 100.1 ± 12.1%, S396/404A transfected: 145.5 ± 12.1%, unpaired t-test $t(11) = 2.2$, $p = 0.040$, Fig.

4b), indicating that tau and its phosphorylation are important for the effect of CORT on LTP. We next wanted to determine whether there was a selective requirement for phosphorylation at either of these sites within this mechanism. We therefore generated and transfected neurons with single phospho-null tau mutants in conjunction with rat tau shRNA. We found that, following CORT treatment, LTP was present in neurons expressing the S396A mutant (untransfected: 84.0± 9.9%; S396A transfected: 177.0 ± 30.4%, unpaired t-test $t(11) = 2.7$, $p = 0.020$, Fig. 4c) but not in neurons expressing the S404A form (untransfected: 101.9 ± 14.2 %; S404A transfected: 108.8± 17.6%, unpaired t-test $t(8) = 0.3$, $p = 0.770$, Fig. 4d). In contrast, neurons where endogenous tau was replaced with Ser199/202/Thr205 residue phospho-null human tau (S/T199/202/205A) were still sensitive to CORT-mediated inhibition of LTP (untransfected: 85.4 ± 13.0%; S/T199/202/205A transfected: 117.4 ± 11.7%, unpaired t-test $t(9) = 1.8$, $p = 0.100$, Fig. 4e). Together, these data suggest that pTau at the Ser396 residue is specifically required for CORT-induced inhibition of LTP.

4. Discussion

Our data are consistent with a serial synaptic weakening mechanism in which the activation of caspase-3 leads to cleavage of Akt1, removing the tonic inhibition of GSK-3, which subsequently increases pTau and causes inhibition of LTP. Caspase-3, GSK-3 and pTau are all critically involved in LTD, and aberrant LTD expression by these molecules has been implicated in the pathophysiology of synapse weakening and neurodegeneration [18,19,21,32-35]. Interestingly, LTP induction can inhibit LTD signalling cascades [17] and, conversely, aberrant activation of LTD and/or synapse

342 weakening signalling cascades inhibits LTP expression [18,19]. This suggests that
343 LTP and LTD signalling molecules are tightly regulated and are maintained in
344 balance at basal states. A given stimuli (i.e., GCs), therefore, could tip this balance in
345 favor of LTP or LTD by acting as a catalyst for signalling mechanisms associated
346 with one or the other form of plasticity. Previous studies have demonstrated that the
347 inhibition of aberrantly expressed LTD and synapse weakening signalling molecules
348 restores LTP expression ordinarily inhibited in an Aβ neurotoxicity model [19,35].
349 Therefore, a compelling explanation for the data presented in this study is that GC-
350 activated synapse weakening signalling results in the inhibition of LTP.

351 Given the numerous studies showing GC-facilitated LTD [11,12,14], there was
352 significant scope for GCs activating key LTD/synapse weakening molecules. Among
353 many of the LTD/synapse weakening molecules, we were specifically interested in
354 GSK-3, considered pivotal in LTD expression and known to be involved in certain
355 types of neurodegeneration [17,36]. Underlying our focus on GSK-3 were the
356 previous observations broadly linking GCs with upregulated GSK-3 activity [31,37],
357 findings which are consistent with the results presented here. A next important step
358 will be to determine the mechanisms by which GCs can modulate GSK-3 activity.
359 GCs activate caspase-3 in cultured rat hippocampal neurons [38] and activation of
360 GR specifically is known to regulate this proapoptotic pathway [39]. Indeed, our
361 TRO-19622 experiment data suggest that GCs regulate the proapoptotic mPTP and
362 cytochrome *c*, and this may serve as a key step in the activation of GSK-3. We have
363 previously suggested that caspase-3-mediated cleavage of Akt-1 is critical for the
364 activation of GSK-3 by Aβ and aberrant expression of LTD in the hippocampus [18].
365 Furthermore, the constitutive inhibition of GSK-3 is primarily governed by the PI3K-
366 Akt signaling pathway [40], which is subject to GC regulation [15,16]. It has also

been suggested that GCs inhibit the canonical wingless (WNT) pathway through Dickkopf 1 (DKK1) [41], which can regulate GSK-3 activity [42]. Therefore, it is clear that signalling pathways converging on GSK-3 are indeed liable to modulation by GCs, and such events could serve as the means by which synapse weakening is induced by GCs.

In the view of activation of GSK-3 by GCs, we hypothesised that the downstream signalling of GSK-3 would promote LTD and/or synapse weakening molecules. Given that GSK-3 is a typical tau kinase and our previous study suggested that tau is essential for LTD expression [20], this hypothesis was tested by knockdown of tau. As we recently found that tau phosphorylation by GSK-3 is a critical molecular step in LTD induction but has no role in LTP [21], we also showed that a specific phospho-null mutation of tau blocked GC-mediated inhibition of LTP. Growing evidence now links GC exposure with tau phosphorylation [31,38,43-46], though the significance of this had remained relatively under explored. Our study now strongly suggests that GC-mediated GSK-3 activation regulates aberrant tau phosphorylation and this causes inhibition of LTP. The real consequences of this could then be two-fold; firstly, the dysregulation of synaptic function as a result of the synapse weakening pathway activation. Secondly, GC-induced tau phosphorylation *per se* could seed tauopathies. It remains to be determined, however, whether there is a specific role of membrane-bound-GRs or cytosolic GRs in activating these signalling pathways that mediate the inhibition of LTP by CORT.

Of particular interest is our novel observation that specific phosphorylation of tau at Ser396 is central to GC-induced synapse weakening. Aside from the established role of this phosphorylation signal with physiological LTD [20,21], it is intriguing to note other studies linking the phosphorylation of tau at this residue with pathological

conditions. In particular, GCs have been shown to induce the accumulation of tau specifically phosphorylated at Ser396 within the synaptic compartment [47]. Furthermore, tau phosphorylated at Ser396 is accumulated in the synaptic compartment of Alzheimer's disease and α-synucleinopathy brains and is considered to be one of the earliest cellular events associated with these pathologies [48,49]. Therefore, the GC-activated caspase-3-GSK-3-pTau signalling pathway may be a potential molecular mechanism of stress mediated synapse weakening that primes neurodegenerative and precedes cognitive decline onset. Control of such aberrant synapse weakening signals may therefore be a useful symptom modification strategy for improvement of cognitive impairments, such as in dementia.

Acknowledgements: K.C., D.W. and P.R. were supported by the BBSRC. J.H.Y. was supported by Korea-UK Alzheimer's research consortium programme under the Korean Ministry of Health and Welfare. Y.S.L. was supported by the London Health Forum under the Korea Health Industry Development Institute, London. C.M.P. was supported by BRACE and Rosetree PhD studentship. K.C. was supported by the Wolfson Research Merit Award and Royal Society, London.

Author Contributions

The study was conceived and designed by K.C. Electrophysiological studies were conducted by J.H.Y., P.R., C.M.P., and biochemical assays were conducted by C.B., G.W., T. P. and Y.S.L. The manuscript was written by D.J.W., P.R., J.H.Y., C.B. and K.C.

References

1. de Kloet, E.R., Joels, M. & Holsboer, F. Stress and the brain: from adaptation to disease. *Nat. Rev. Neurosci*. **6**, 463-75 (2005).

2. Lupien, S.J. et al. Cortisol levels during human aging predict hippocampal atrophy and memory deficits. *Nat. Neurosci*. **1**, 69-73 (1998).

3. Starkman, M.N., Gebarski, S.S., Berent, S. & Schteingart, D.E. Hippocampal formation volume, memory dysfunction, and cortisol levels in patients with Cushing's syndrome. *Biol. Psychiatry*. **32**, 756-65 (1992).

4. Sapolsky, R.M., Romero, L.M. & Munck, A.U. How do glucocorticoids influence stress responses? Integrating permissive, suppressive, stimulatory, and preparative actions. *Endocr. Rev.* **21**, 55-89 (2000).

5. Cho, K. Chronic 'jet lag' produces temporal lobe atrophy and spatial cognitive deficits. *Nat. Neurosci*. **4**, 567-8 (2001).

6. Newcomer, J.W., Craft, S., Hershey, T., Askins, K. & Bardgett, M.E. Glucocorticoid-induced impairment in declarative memory performance in adult humans. *J. Neurosci*. **14**, 2047-53 (1994).

7. Kirschbaum, C., Wolf, O.T., May, M., Wippich, W. & Hellhammer, D.H. Stress- and treatment-induced elevations of cortisol levels associated with impaired declarative memory in healthy adults. *Life Sci*. **58**, 1475-83 (1996).

8. Conrad, C.D., Galea, L.A., Kuroda, Y. & McEwen, B.S. Chronic stress impairs rat spatial memory on the Y maze, and this effect is blocked by tianeptine pretreatment. *Behav. Neurosci*. **110**, 1321-34 (1996).

9. Sousa, N., Lukoyanov, N.V., Madeira, M.D., Almeida, O.F. & Paula-Barbosa, M.M. Reorganization of the morphology of hippocampal neurites and synapses after stress-induced damage correlates with behavioral improvement. *Neuroscience*. **97**, 253-66 (2000).

10. de Quervain, D.J., Aerni, A., Schelling, G. & Roozendaal, B. Glucocorticoids and the regulation of memory in health and disease. *Front. Neuroendocrinol.* **30**, 358-70 (2009).

11. Kim, J.J., Foy, M.R. & Thompson, R.F. Behavioral stress modifies hippocampal plasticity through N-methyl-D-aspartate receptor activation. *Proc. Natl. Acad. Sci. U S A.* **93**, 4750-3 (1996).

12. Xu, L., Anwyl, R. & Rowan, M.J. Behavioural stress facilitates the induction of long-term depression in the hippocampus. *Nature*. **387**, 497-500 (1997).

13. Nabavi, S. et al. Engineering a memory with LTD and LTP. *Nature*. **511**, 348-52 (2014).

14. Yang, C.H., Huang, C.C. & Hsu, K.S. Behavioral stress modifies hippocampal synaptic plasticity through corticosterone-induced sustained extracellular signal-regulated kinase/mitogen-activated protein kinase activation. *J. Neurosci.* **24**, 11029-34 (2004).

15. Jeanneteau, F., Garabedian, M.J. & Chao, M.V. Activation of Trk neurotrophin receptors by glucocorticoids provides a neuroprotective effect. *Proc. Natl. Acad. Sci. U S A*. **105**, 4862-7 (2008).

16. Yang, S., Roselli, F., Patchev, A.V., Yu, S. & Almeida, O.F. Non-receptor-tyrosine kinases integrate fast glucocorticoid signaling in hippocampal neurons. *J. Biol. Chem.* **288**, 23725-39 (2013).

17. Peineau, S. et al. LTP inhibits LTD in the hippocampus via regulation of GSK3beta. *Neuron*. **53**, 703-17 (2007).

18. Li, Z. et al. Caspase-3 activation via mitochondria is required for long-term depression and AMPA receptor internalization. *Cell.* **141**, 859-71 (2010).

19. Jo, J. et al. Abeta(1-42) inhibition of LTP is mediated by a signaling pathway involving caspase-3, Akt1 and GSK-3beta. *Nat. Neurosci*. **14**, 545-7 (2011).

20. Kimura, T. et al. Microtubule-associated protein tau is essential for long-term depression in the hippocampus. *Philos. Trans. R. Soc. Lond. B. Biol. Sci*. **369**, 20130144 (2014).

21. Regan, P. et al. Tau phosphorylation at serine 396 residue is required for hippocampal LTD. *J. Neurosci*. **35**, 4804-12 (2015).

22. Shipton OA, et al. Tau protein is required for amyloid {beta}-induced impair-ment of hippocampal long-term potentiation. *J Neurosci* **31**, 1688-92 (2011).

23. Ittner, L.M. & Gotz, J. Amyloid-beta and tau--a toxic pas de deux in Alzheimer's disease. *Nat. Rev. Neurosci*. **12**, 65-72 (2011).

24. Sotiropoulos, I. & Sousa, N. Tau as the Converging Protein between Chronic Stress and Alzheimer's Disease Synaptic Pathology. *Neurodegener. Dis*. **16**, 22-5 (2016).

477 25. Stoppini, L., Buchs, P.A. & Muller, D. A simple method for organotypic
478 cultures of nervous tissue. *J. Neurosci. Methods*. **37**, 173-82 (1991).

479 26. Lo, D.C., McAllister, A.K. & Katz, L.C. Neuronal transfection in brain slices
480 using particle-mediated gene transfer. *Neuron*. **13**, 1263-8 (1994).

481 27. Garrido, C. et al. Mechanisms of cytochrome c release from mitochondria.
482 *Cell Death Differ*. **13**, 1423-33 (2006).

483 28. Liao, Y. & Hung, M.C. Physiological regulation of Akt activity and stability. *Am*
484 *J. Transl. Res.* **2**, 19-42 (2010).

485 29. Alessi DR, et al. Mechanism of activation of protein kinase B by insulin and
486 IGF-1. *EMBO J* **15**, 6541-6551 (1996).

487 30. Mandelkow EM, et al. Glycogen synthase kinase-3 and the Alzheimer-like
488 state of microtubule-associated protein tau. *FEBS Lett* **314**, 315-21. (1992).

489 31. Sotiropoulos, I. et al. Stress acts cumulatively to precipitate Alzheimer's
490 disease-like tau pathology and cognitive deficits. *J. Neurosci.* **31**, 7840-7
491 (2011).

492 32. Regan, P., Whitcomb, D.J. & Cho, K. Physiological and Pathophysiological
493 Implications of Synaptic Tau. *The Neuroscientist.* 1-15. (2016).

494 33. Regan, P., Hogg, E., Whitcomb, D.J. & Cho, K. Long-term depression: a new
495 conceptual understanding of Alzheimer's disease. *Eur. J. Neurodegener. Dis*.
496 **2**, 79-89 (2014).

497 34. Carroll, J.C. et al. Chronic stress exacerbates tau pathology,
498 neurodegeneration, and cognitive performance through a corticotropin-

releasing factor receptor-dependent mechanism in a transgenic mouse model of tauopathy. *J. Neurosci*. **31**, 14436-49 (2011).

35. Kailainathan et al. Activation of a synapse weakening pathway by human Val 66 but not Met66 pro-brain-derived neurotrophic factor (proBDNF). *Pharmacol Res* **104**, 97-107 (2015).

36. Lei, P., Ayton, S., Bush, A.I. & Adlard, P.A. GSK-3 in Neurodegenerative Diseases. *Int. J. Alzheimers Dis*. 2011, 189246 (2011).

37. Sotiropoulos, I. et al. Glucocorticoids trigger Alzheimer disease-like pathobiochemistry in rat neuronal cells expressing human tau. *J. Neurochem.* **107**, 385-97 (2008).

38. Liu, B. et al. Neuroprotective effects of icariin on corticosterone-induced apoptosis in primary cultured rat hippocampal neurons. *Brain Res.* **1375**, 59-67 (2011).

39. Crochemore, C. et al. Direct targeting of hippocampal neurons for apoptosis by glucocorticoids is reversible by mineralocorticoid receptor activation. *Mol. Psychiatry.* **10**, 790-8 (2005).

40. Doble, B.W. & Woodgett, J.R. GSK-3: tricks of the trade for a multi-tasking kinase. *J. Cell Sci*. **116**, 1175-86 (2003).

41. Matrisciano, F. et al. Induction of the Wnt antagonist Dickkopf-1 is involved in stress-induced hippocampal damage. *PLoS One*. 6, e16447 (2011).

42. Metcalfe, C. & Bienz, M. Inhibition of GSK3 by Wnt signalling--two contrasting models. *J. Cell Sci.* **124**, 3537-44 (2011).

521 43. Cuadrado-Tejedor, M. et al. Chronic mild stress in mice promotes cognitive
522 impairment and CDK5-dependent tau hyperphosphorylation. *Behav. Brain*
523 *Res.* **220**, 338-43 (2011).

524 44. Liu, Y. et al. Tau phosphorylation and mu-calpain activation mediate the
525 dexamethasone-induced inhibition on the insulin-stimulated Akt
526 phosphorylation. *PLoS One.* 7, e35783 (2012).

527 45. Zhang, L.F. et al. Increased hippocampal tau phosphorylation and axonal
528 mitochondrial transport in a mouse model of chronic stress. *Int. J*
529 *Neuropsychopharmacol.* **15**, 337-48 (2012).

530 46. Joshi, Y.B., Chu, J. & Pratico, D. Stress hormone leads to memory deficits
531 and altered tau phosphorylation in a model of Alzheimer's disease. *J*
532 *Alzheimers Dis.* **31**, 167-76 (2012).

533 47. Pinheiro, S. et al. Tau Mislocation in Glucocorticoid-Triggered Hippocampal
534 Pathology. *Mol. Neurobiol.* **53**, 4745-53 (2016).

535 48. Muntane, G., Dalfo, E., Martinez, A. & Ferrer, I. Phosphorylation of tau and
536 alpha-synuclein in synaptic-enriched fractions of the frontal cortex in
537 Alzheimer's disease, and in Parkinson's disease and related alpha-
538 synucleinopathies. *Neuroscience*. **152**, 913-23 (2008).

539 49. Mondragon-Rodriguez, S., Perry, G., Luna-Munoz, J., Acevedo-Aquino, M.C.
540 & Williams, S. Phosphorylation of tau protein at sites Ser(396-404) is one of
541 the earliest events in Alzheimer's disease and Down syndrome. *Neuropathol.*
542 *Appl. Neurobio.l* **40**, 121-35 (2014).

Figure Legends

Figure 1: Glucocorticoids impair LTP via caspase-mediated GSK-3 activation

(**a**, **b, c and d**) Field recording in rat hippocampus CA1. *Top*: Example traces of fEPSPs from indicated timepoints. *Bottom*: Mean fEPSP slope shown as percentage of the established baseline. (**a**) LTP is inhibited by CORT treatment (n = 8). (**b**) Bath application of DEX inhibits LTP (n = 6). (**c**) Treatment with CT-99021 prevents LTP impairment induced by CORT (n = 6). (**d**) Z-DEVD-FMK blocks impairment of LTP by CORT (n = 6), but scrambled peptide Z-FA-FMK does not (n = 6). Bath application of CORT and CT-99021, and delivery of tetanus (100Hz, 100 pulses) indicated by black rectangles. (**e**) Z-DEVD-FMK rescues the reduction of GSK-3 inhibitory phosphorylation caused by CORT treatment (n = 10), but Z-FA-FMK does not (n = 10). *Left*: Cropped example blots showing immunoreactive bands from different treatment groups. *Top Right*: Quantification of changes in immunoreactivity of pS9 GSK-3β normalised against total GSK-3β. *Bottom Right*: Levels of total GSK-3β normalised against β-actin loading control. (**f**, **g** and **h**) Whole cell patch clamp recording in CA1 region of cultured hippocampal slices. *Top*: Example traces of EPSCs from indicated timepoints. *Bottom*: Mean peak EPSC shown as percentage of the established baseline. (**f**) CORT treatment blocks LTP induction (n = 5, control n = 5). (**g**) GR shRNA prevents CORT-induced LTP impairment (GR shRNA transfected n = 5, untransfected n = 5). (**h**) XIAP Bir1,2 prevents CORT-induced LTP impairment (XIAP Bir1,2 transfected n = 7, untransfected n = 6). All bars and circles represent the mean ± SEM. Statistical significance was determined by one-way ANOVA and Holm-Sidak post hoc analysis indicated as $*p < 0.05$, $**p < 0.01$, $***p < 0.001$.

Figure 2: Caspase-mediated Akt1 cleavage is required for the inhibition of LTP by CORT

(**a**) TRO-19622 prevents the reduction of pS9GSK-3β caused by CORT treatment (*n* = 6). *Left*: Cropped example blots showing immunoreactive bands from different treatment groups. *Top Right*: Quantification of changes in immunoreactivity of pS9 GSK-3β normalised against total GSK-3β. *Bottom Right*: Levels of total GSK-3β normalised against β-actin loading control. (**b**) TRO-19622 inhibits CORT-induced LTP impairment (*n* = 6). (**c**) *Left*: Cropped example blots showing immunoreactive bands from different treatment groups. *Middle*: Quantification of pAkt1(Thr308) immunoreactivity normalised to total Akt1. *Right*: Total Akt1 normalised to β-actin loading control. The reduction in Thr308 phosphorylation of Akt1 following CORT treatment (*n* = 6) was rescued by Z-DEVD-FMK (*n* = 6) and RU486 (*n* = 6). (**d**) CORT treatment reduces Akt1 activity as determined by a significant decrease in pGSKαβ Ser21/9 levels compared to control (*n* = 3). (**e** and **f**) Whole cell patch clamp recording in CA1 region of cultured hippocampal slices. *Top*: Example traces of EPSCs from indicated timepoints. *Bottom*: Mean peak EPSC shown as percentage of the established baseline. (**e**) CORT does not impair LTP in slices transfected with Akt1 triple mutant (Akt1 triple mutant transfected *n* = 6, untransfected *n* = 5), (**f**) whereas Akt1 wild-type has no effect on CORT-induced LTP impairment (Akt1 wild-type *n* = 7, untransfected *n* = 6). 2 Hz stimulation indicated by black rectangles. All bars and circles represent the mean ± SEM. Statistical significance was determined by one-way ANOVA and Holm-Sidak post hoc analysis and unpaired t-test indicated as $*p < 0.05$, $**p < 0.01$, $***p < 0.001$.

Figure 3: Caspase, mPTP and GSK-3 activation regulate CORT-mediated changes to pTau

Western blots showing changes in phosphorylation of tau. *Left*: Cropped example blots showing immunoreactive bands from different treatment groups. *Right*: Quantification of pTau antibody immunofluorescence normalised to total tau (Tau5). (**a** and **b**) pTau measured by PHF-1 is increased by CORT and rescued by Z-DEVD-FMK, but not scrambled peptide Z-FA-FMK (n = 6). Immunoreactivity of AT8 is unchanged by any treatment (n = 6). (**c** and **d**) TRO-19622 also prevents the increase in PHF-1 immunoreactivity caused by CORT (n = 6), without affecting levels of AT8 (n = 6). (**e** and **f**) Additionally, CT-99021 blocks the increase in PHF-1 immunoreactivity caused by CORT (n = 9), while AT8 immunoreactivity is not affected by CORT or CT-99021 (n = 9). All bars represent the mean ± SEM. Statistical significance was determined by one-way ANOVA and Holm-Sidak post hoc analysis indicated as *p < 0.05, **p < 0.01, ***p < 0.001.

Figure 4: pTau at Ser396 is specifically required for CORT-induced inhibition of LTP

Whole cell patch clamp recording in CA1 region of cultured hippocampal slices. *Top*: Example traces of EPSCs from indicated timepoints. *Bottom*: Mean peak EPSC shown as percentage of the established baseline. (**a**) LTP can still be induced after CORT treatment in neurons transfected with tau shRNA (tau shRNA n = 8, untransfected n = 6). (**b**) Neurons expressing the tau S396/404A mutant exhibited LTP after treatment with CORT (tau S396/404A transfected n = 8, untransfected n = 5). (**c**) LTP can be induced after CORT treatment in neurons transfected with the

single residue S396A tau mutant (tau S39A transfected *n* = 7, untransfected *n* = 6). (**d**) CORT impairs LTP in neurons expressing tau S404A (tau S404A transfected *n* = 5, untransfected *n* = 5). (**e**) The tau S/T 199/202/205A mutant was unable to prevent inhibition of LTP by CORT (tau S/T 199/202/205A transfected *n* = 6, untransfected *n* = 5). 2Hz stimulation indicated by black rectangles. All bars and circles represent the mean ± SEM. Statistical significance was determined by unpaired t-test.

Figures

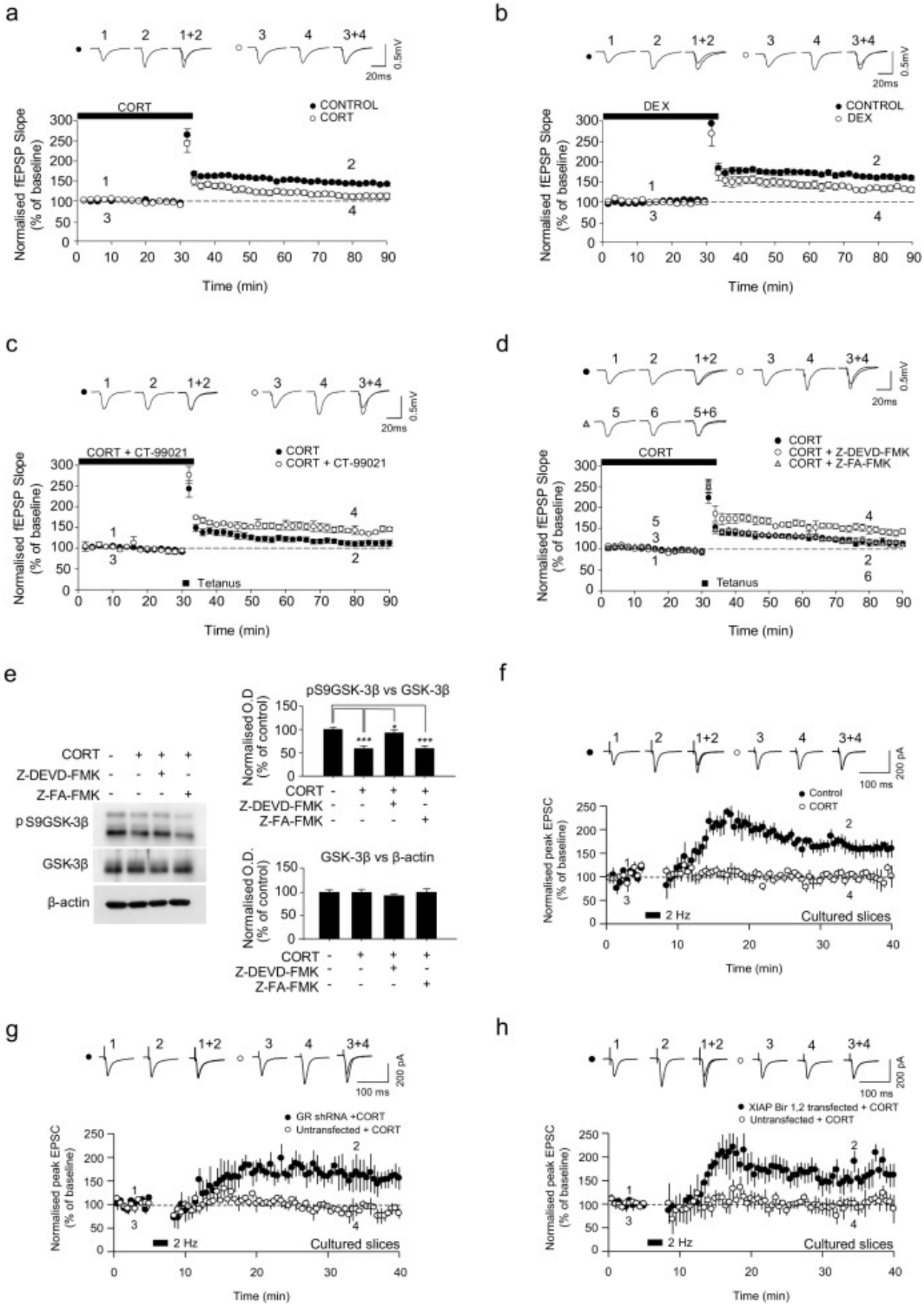

Fig. 1. Glucocorticoids impair LTP *via* caspase-mediated GSK-3 activation.

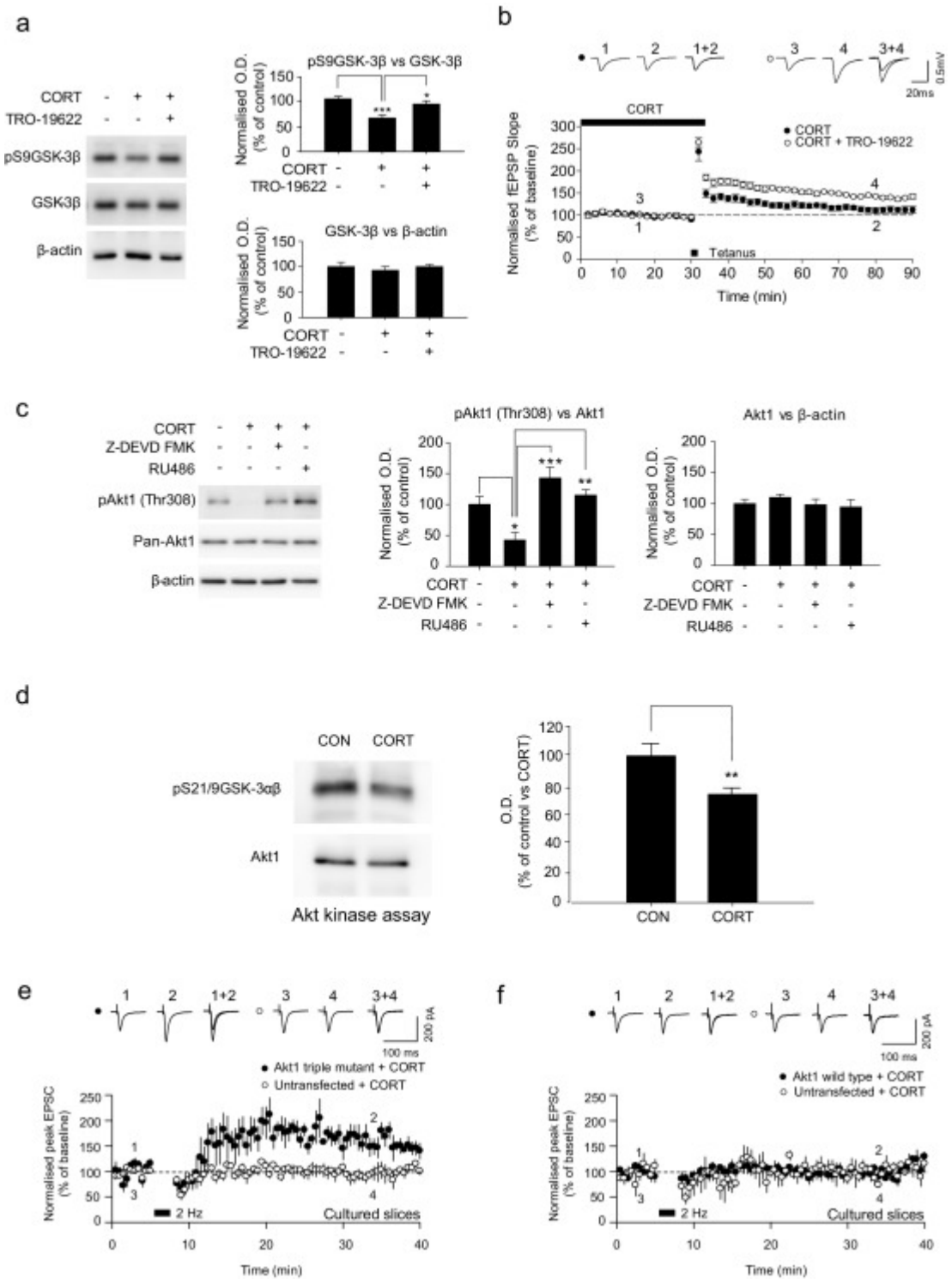

Fig. 2. Caspase-mediated Akt1 cleavage is required for the inhibition of LTP by CORT.

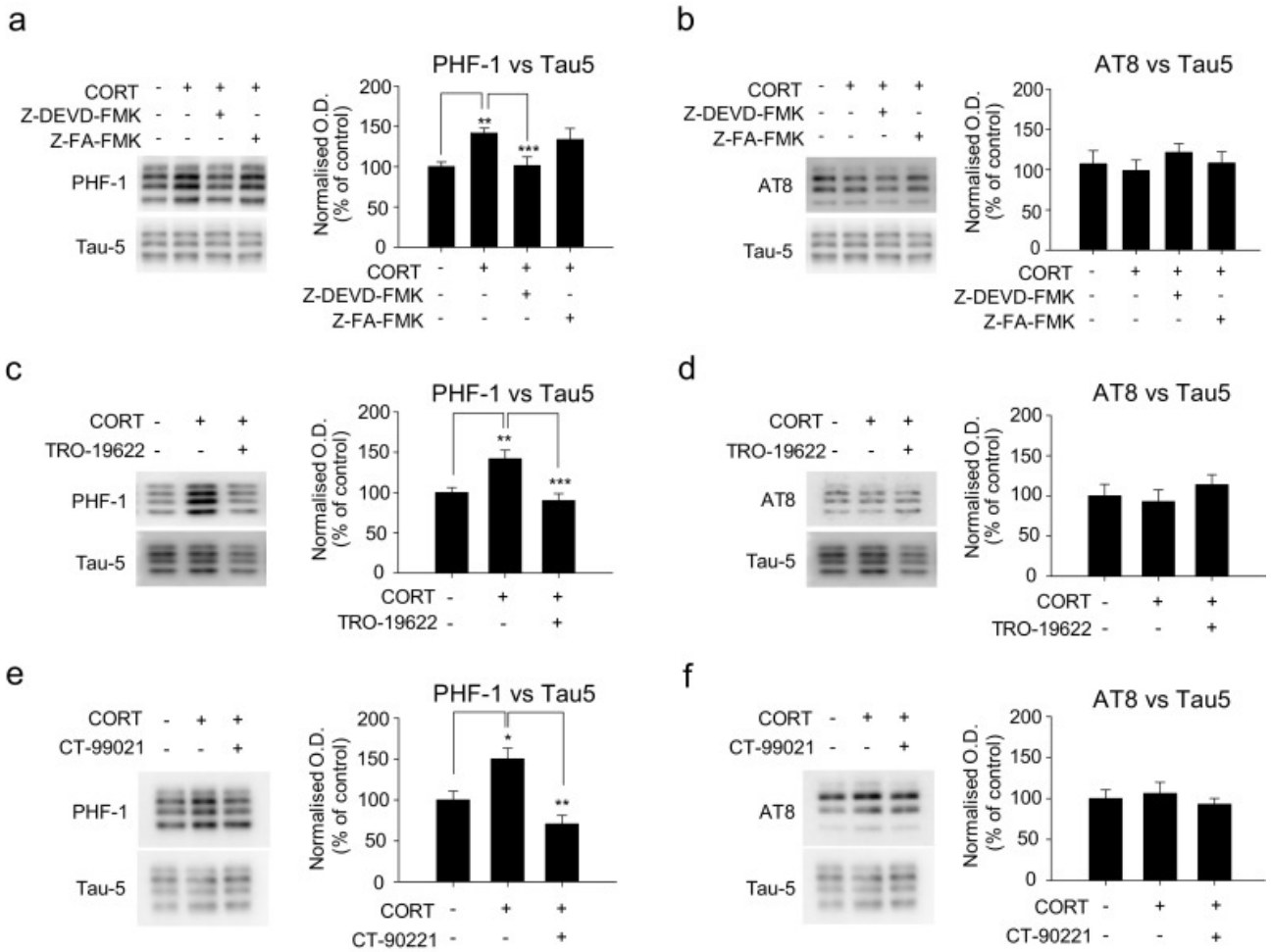

Fig. 3. Caspase, mPTP and GSK-3 activation regulate CORT-mediated changes to pTau.

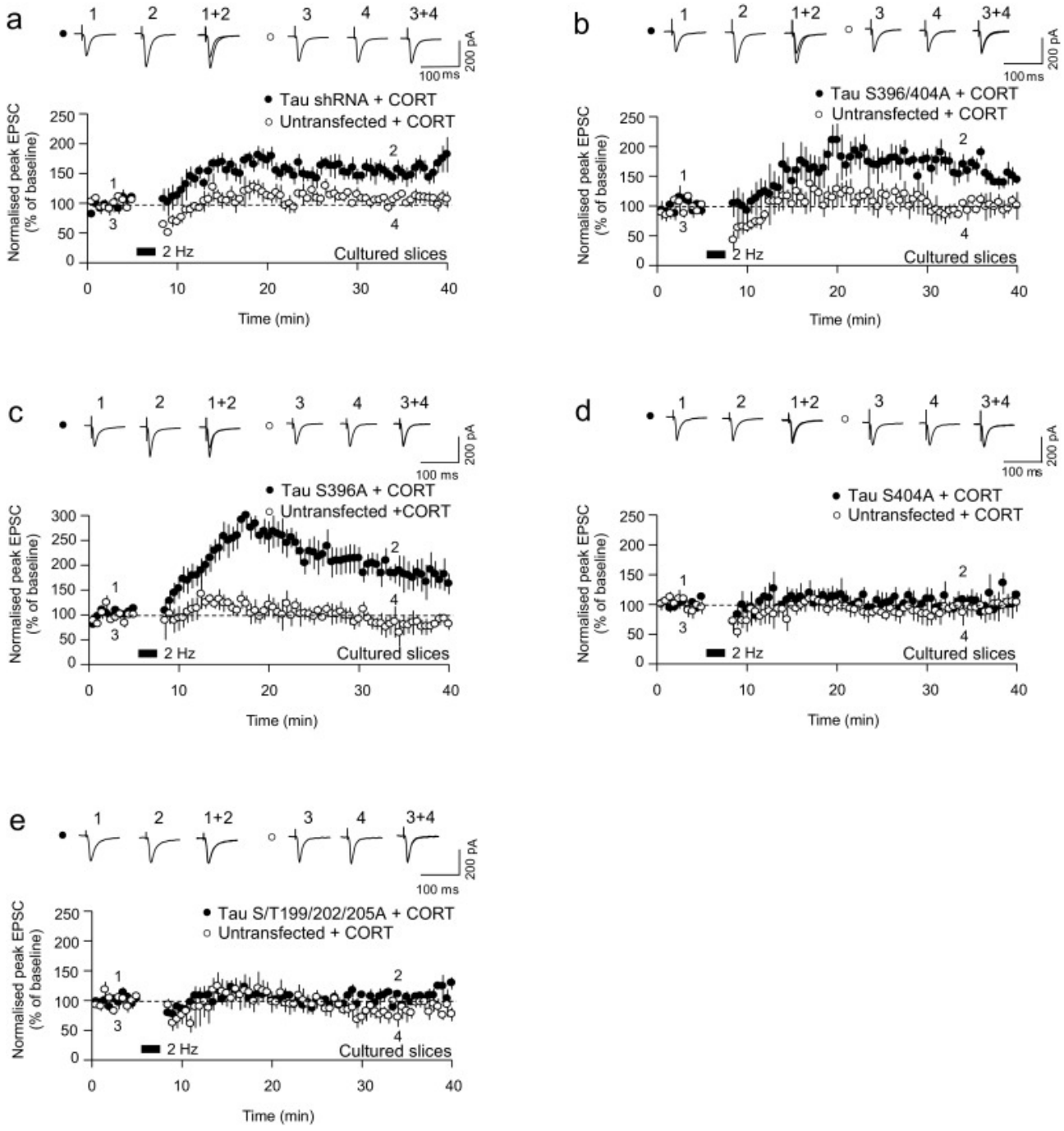

Fig. 4. pTau at Ser396 is specifically required for CORT-induced inhibition of LTP.